

Enhancing UAV Communication Performance: Analysis Using Interference Based Geometry Stochastic Model and Successive Interference Cancellation

Emmanuel Ampoma Affum[1(✉)], Matthew O. Adigun[2], Kofi Anane Boateng[1], Sunday Adeola Ajagbe[3], and Emmanuel Addo[1]

[1] Department of Telecommunication Engineering, Kwame Nkrumah University of Science and Technology, Kumasi, Ghana
eaffum.coe@knust.edu.gh, kaboateng10@st.knust.edu.gh
[2] Department of Computer Science, University of Zululand, Richards Bay, South Africa
adigunm@unizulu.ac.za
[3] Computer Engineering Department, Ladoke Akintola University of Technology, Ogbomoso, Nigeria
saajagbe@pgschool.lautech.edu.ng

Abstract. The reliability and transmission quality in any wireless communication network is paramount. Unmanned Aerial Vehicle (UAV) communication networks are no exception to this fact. Hence, the need to investigate various communication technologies that will improve and be able to support the various applications of the UAV communication network. Correlated based stochastic models (CBSM) have been used to assess theoretical performances in UAV communication networks. CBSM has insufficient precision in a practical system. Geometry based stochastic channel models (GBSM) on the other hand, displays realistic channel features. These realistic channel features include pathloss, angle of arrival (AoA), angle of departure (AoD), etc. GBSM is better and ideal for channel modeling. This paper analyses the UAV communication networks in terms of their reliability and quality in transmission. MIMO-OFDM technology has been proposed to improve the UAV communication network. In this UAV network, the transmitters are modeled as cylindrical array (CA) because of its attribute of good regulation in 3-D space among others. A 3-D GBSM is proposed in the analysis. Also, an interference model has been presented in the UAV communication network. Results from this research show that MIMO-OFDM improves the reliability and quality of the UAV communication network. Generally, the capacity and BER increased with increasing number of antennas and SINR. However, beyond SINR of $25dB$, we observed an irreducible error floor, that is, BER remained constant with increasing SINR. Successive Interference Cancellation (SIC) was therefore employed to minimize the irreducible error floor in the UAV communication network. This increased the average capacity and BER to about $25bits/s/Hz$ and 10^{-8} respectively.

© The Author(s), under exclusive license to Springer Nature Switzerland AG 2022
O. Gervasi et al. (Eds.): ICCSA 2022, LNCS 13375, pp. 232–245, 2022.
https://doi.org/10.1007/978-3-031-10522-7_17

Keywords: UAV communication networks · MIMO-OFDM · Cylindrical array · CBSM · GBSM · Successive interference cancellation

1 Introduction

Unmanned Aerial Vehicles (UAVs), often known as drones, are airplanes that do not have any human passengers on board. They are set up to be totally or partially self-contained. Even though UAVs are classed based on their application and Quality of Service (QoS), they are commonly categorized based on their altitude and wing type [1–3]. UAV communication network comprises a drone, a base station, and a communication link between the UAV and the base station (BS). UAVs have a broad range of applications that include precision agriculture, disaster management, monitoring and surveillance, aerial photography, military applications, telecommunications, delivery of medical supplies, and rescue operations [4–8].

1.1 Related Works

With the broad and diverse applications of UAV communication in our world, there is the need to ensure efficiency and reliability in the UAV network communication link. This has been the recent focus of researchers regarding UAV communication networks. Given this, authors in [9,10] presented on Orthogonal Frequency Division Multiplexing (OFDM)and Single Carrier-Frequency Division Multiplexing (SC-FDM) in improving the communication link. This is because of the prominent resilience they have with regards to multipath distortion and higher throughput and likely data rates as compared to the traditional spread spectrum technology being currently employed in the UAV communication network. SC-FDM and OFDM improved the UAV communication network. However, in [9,10], correlated based stochastic channel models (CSBM) were used for the analysis. The accuracy of CSBM is insufficient for practical systems, therefore they are used to analyze theoretical performance. These realistic features include pathloss, AoA, AoD, etc.

Again, authors in [11–16] have considered Massive Multiple Input Multiple Output (mMIMO) in the UAV communication network under realistic 3GPP assumptions. The multi-user mode was compared to the typical single-user mode, and the multi-user mode significantly increased the channel and control (C&C) capacity. However, with mMIMO, as the number of transmit antennas increases, the pilot overhead for channel estimate becomes excessively large, which is an issue in wireless communication [17]. To reduce the channel estimation overhead, authors in [18] used time division duplex (TDD) communication. Where the downlink (DL) and channel state information (CSI) can be attained from that of the uplink (UL) channel by utilizing channel reciprocity. Another way

is to employ frequency division duplex (FDD) which is more efficient compared with TDD. Authors in [19], presented the use of MIMO-OFDM in the UAV communication networks as MIMO will decrease the effect of multipath fading without expanding power, sacrificing bandwidth, and also utilize channel capacity. MIMO can viably defeat issues of limited capacity and low transmission rate of UAV communication [20]. OFDM on the other hand mitigates frequency selective fading [21] which is a problem associated with the MIMO system [22]. MIMO-OFDM improves the capacity and also effectively overcomes frequency selective fading which improves the data transmission quality and reliability [23]. However, in this literature, small antenna scale and a correlated based channel model were considered for analysis.

1.2 Motivation

In comparison to prior research on UAV communication networks [9,11,19], having a realistic study that takes into account the diverse uses of UAV communication over a cellular network presents additional challenges. To begin, the channel model between the UAV and the ground station (base station) will no longer follow correlated based stochastic channel models (CBSM) but will instead be geometry based stochastic channel models (GBSM). CBSM analyses are theoretical and offer less precision in a communication system. GBSM on the other hand displays realistic channel features which consider pathloss, AoA, AoD, etc. Despite the additional processing complexity, this is better for channel modeling [24]. Second, because the UAV communication network will be deployed over a shared frequency band with other cellular networks, interference concerns may arise. Previous research on UAV communication networks, such as [11–17], have not considered both the first and second issues. In this literature, we looked into these issues and their trade-offs. This work will, to the best of our knowledge, offer *analysis of the performance of UAV communication in MIMO-OFDM in the presence of interference using GBSM.*

1.3 Contribution

The main contribution of this paper is to present and analyze UAV communication regarding GBSM between the UAV and the CA MIMO-OFDM BS. We considered the WINNER+ channel model standard in [25] that follows GBSM and present a new channel realization when the transmitter is modeled as CA. Here, the BS of the UAV communication network is modeled as a cylindrical array (CA). CA is considered because the emitted MIMO signals from these arrays can be well controlled in 3-D space increasing system capacity [26,27]. Additionally, the CA enables the generation of focused beams in any horizontal direction or an omnidirectional pattern in the horizontal plane [28]. Furthermore, the CA can be used to minimize clutter by using scanning acceleration

and space-time signal processing [29]. In addition, we investigate the impact of interference on MIMO-OFDM in UAV communication networks. We considered several UAVs that support downlink transmission to several user equipments (UE) and CA MIMO-OFDM base stations. The contributions of this paper have been summarized as follows:

1. We modeled the base station (BS) as a cylindrical array (CA) and presented a new channel model based on GBSM for the MIMO-OFDM system in the UAV communication network.
2. We presented an interference model and incorporated the model into the channel to see the impact of interference on the UAV communication network.
3. We considered successive interference cancellation at the receiver in the proposed UAV communication network. When SIC is used, it enables the user to uniquely decode the data being received with minimal interference and data loss.
4. We present results to show that the capacity and BER generally increase with increase in the number of antennas and SINR. Here, beyond SINR of $25dB$, the BER of the network remains constant with increasing SINR. This is known as the irreducible error floor. We then present on SIC to reduce the irreducible error floor.

2 The System Model

2.1 Proposed UAV System Model

In this section, we discuss the various aspect of the UAV communication network and how they are linked to form the system model. We considered a circular area with UAVs deployed for an application. For this network, the following scenarios were considered: communication between the user equipment and the UAV, communication between the UAV and base stations, and communication between the base stations and the UEs. All base stations within this network are considered to be MIMO-OFDM transceivers with their antennas modeled as cylindrical array (CA). Here we looked at the downlink scenario. Also, base stations are located at a fixed distance from each other as shown in Fig. 1.

2.2 Proposed Interference Model

In this section, we examine the various interference that can be experienced by all the systems within this network considering the downlink scenario. Based on this, an appropriate Signal-to-Interference-plus noise ratio (SINR) was established. As shown in the diagram in Fig. 2, the received signal at the base stations consists of the intended signal from the UAV transmitter as well as interference from other UAVs and MIMO-OFDM transmitters. On the other hand, the UE receives the

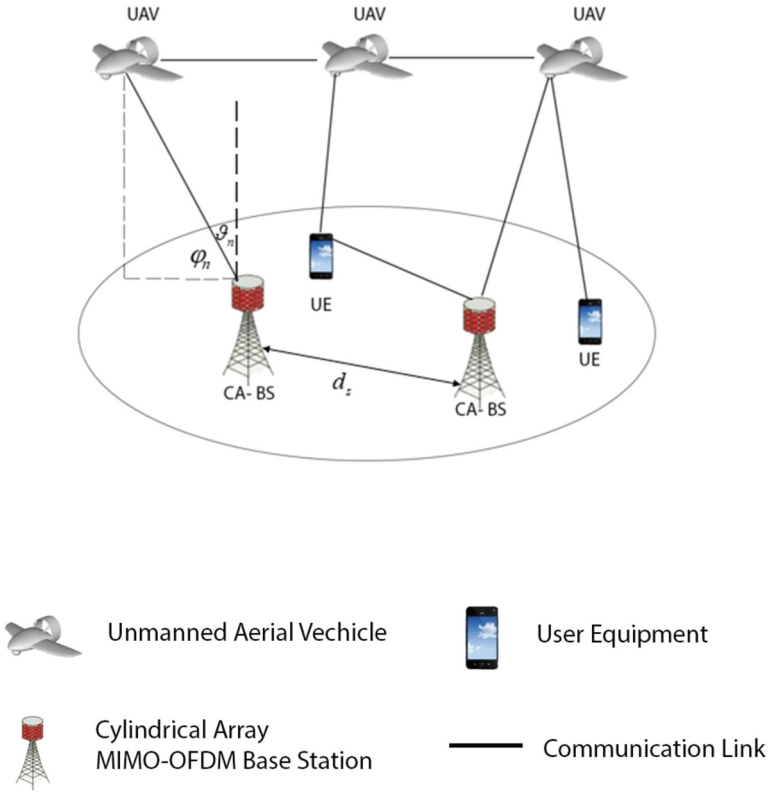

Fig. 1. UAV system model including UAVs, UEs, and CA MIMO-OFDM base stations (CA-BS)

intended signal from the UAV but is also subjected to interference from all other MIMO-OFDM transmitters. The interference expression is given as [30]:

$$I = p_i \sum_{i \in k} \xi_i^2 \Upsilon_i^{-v} \tag{1}$$

where ξ_i is the fading amplitude of the ith interfering signal. All interfering signals are considered to be sent at the same power level p_i [30], however, pathloss and fading occur in a mutually independent manner. In addition, it is assumed that the interferers are independent and identically distributed (i.i.d). Also, Υ_i represents the distance between the interfering terminal i and the receiver, while v represents the pathloss exponent in the receiver's environment. The output signal-to-interference-plus-noise ratio (SINR)expression as:

$$\gamma = \frac{p_s \alpha_s^2 d_s^{-v}}{N_o + I} \tag{2}$$

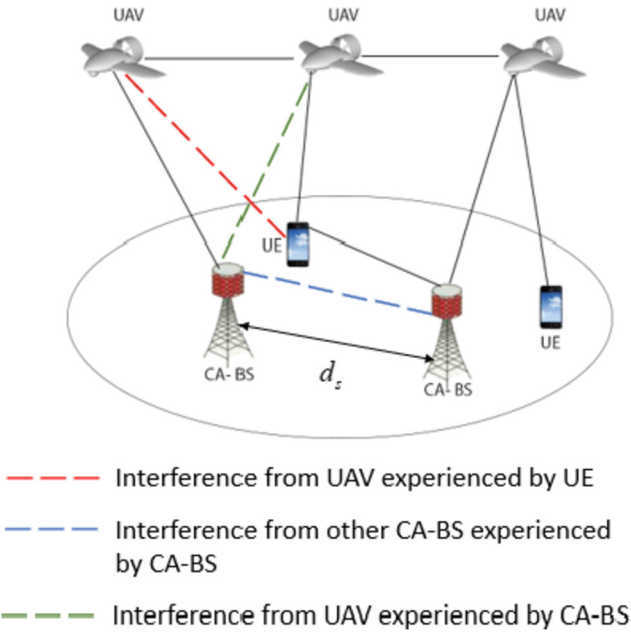

Fig. 2. Interference model showing interference among UAVs, UEs and CA-BSs

where p_s is the transmitting power of the desired signal, d_s is the distance between the transmitter and the receiver, α_s is the Rayleigh-faded amplitude of the desired signal. I represents the interference being experienced by the BS.

2.3 The Channel Model

In this section, we examined the GBSM standards and the WINNER+ model in [31] and [32], which follows a GBSM approach and presented a relating channel realization between the BS when modeled as CA and the UAV. We considered these WINNER+ and 3GPP standards because it has a substantial component of energy that is radiated in the elevation according to research. Therefore, in the azimuth, the propagation path does not enhance performance [33]. For the 3D MIMO-OFDM analysis, we represent the BS as CA. However, the UAV is represented by summing contributions of N multiple paths with channel parameters such as delay, power, and both azimuthal and elevation spread. In [25], authors defined the effective channel between the sth transmitting UAV and the uth receiving BS as:

$$[H_{s,u}] = \sum_{n=1}^{N} \alpha_n \sqrt{g_t(\phi_n, \theta_n, \theta_{tilt})} \sqrt{g_r(\varphi_n, \vartheta_n)} \times [\alpha_n(\varphi_n, \vartheta_n)]_u \times [\alpha_t(\phi_n, \theta_n)] \quad (3)$$

where $s = 1, ..., N_{UAV}, u = 1, ..., N_{BS}, \alpha_n$ is the complex amplitude of the nth path, (ϕ_n, θ_n) are the azimuth and the elevation angles-of-departure (AODs)

respectively. (φ_n, ϑ_n) are the azimuth and elevation of angles of arrival (AOAs) of the nth path respectively. Following the procedures of ITU and 3GPP standards, the gain of each antenna array at the BS is expressed as $g_t(\phi_n, \theta_n, \theta_{tilt}) \approx g_t, H(\phi_n g_t, v(\theta_n, \theta_{tilt}))$. The antenna array responses are represented by $\alpha_t(\phi, \theta)$ and $\alpha_r(\phi, \theta)$.

Different transmission modes indicated in [27] and [34] are required with the use of CA antenna ports. With this antenna arrangement, each antenna port appears to be a single port since all of its components convey the same signal. The response of the *uth* UAV antenna in relation to the 3-D channel model is expressed as [34].

$$[\alpha_r(\phi_n, \theta_n)]_s = \exp(ik(u-1)d_r \sin\theta_n \sin\vartheta) \tag{4}$$

Also the array response of the *sth* BS antenna of CA using Eq. (3) can be expressed as

$$[\alpha_t(\phi_n, \theta_n)]_s = \exp(ik\rho(4\lambda(m-1)/M)\cos(\phi_n - \varphi_s)\sin\theta_n) \tag{5}$$

The resulting 3-D channel realization between the *sth* transmit antenna of the CA and the single receiving antenna can be expressed as

$$[H_{s,u}]_{CA} = \sum_{n=1}^{N} \alpha_n \sqrt{g_t(\phi_n, \theta_n, \theta_{tilt})} \times \exp(ik\rho(4\lambda(m-1)/M)\cos(\phi_n - \varphi_s)\sin\theta_n)$$

$$\times \sqrt{g_r(\varphi_n, \vartheta_n)} \times \exp(ik(u-1)d_r \sin\theta_n \sin\vartheta) \tag{6}$$

where k is the wave number, d_r is the separation between the receiving antennas, $\rho = 4\lambda/l$ which represents the radius of the cylinder. $m = 1, ..., M$ is the total number of UCA elements within the CA in the z-direction.

2.4 The MIMO-OFDM System Model

In this section, we dicuss the MIMO-OFDM system model in the network. Here, we assumed that the system has N_t transmitting antennas and N_r receiving antenna. By transforming serial streams to parallel streams using space-time pre-processing, the serial information bit stream is transformed into N_t sub-data streams. After being OFDM modulated, the sub-data streams are transmitted simultaneously by N_t antennas. If the OFDM system contains N carriers, then there will be a total of $N_t N$ OFDM samples in one OFDM symbol period. The $N_t \times N$ samples sent by the *nth* OFDM symbol period is represented by x_n. Where x_n is an $N_t \cdot N$ dimensional column vector. We represent the received OFDM signal as y_n. Where y_n is an $(N+N_g+I)\cdot N_r$ dimensional column vector. Where N_g represent additive white Gaussian noise and I the interference within the channel. The total number of OFDM symbols being transmitted can be expressed as [19]

$$x_n = \left[x_{1,n}^T, x_{2,n}^T, ..., x_{N,n}^T\right]^T \tag{7}$$

with a corresponding received signal expressed as

$$y_n = \left[y_{1,n}^T, y_{2,N}^T, ..., y_{N,n}^T\right]^T \tag{8}$$

When perfect synchronization is achieved at the receiver, the MIMO-OFDM system's input and output relationship may be described in the matrix form below

$$\bar{y} = \bar{H}x + \bar{n} + \bar{I} \tag{9}$$

where $\bar{y}$ is a $N \cdot N_r$ dimensional column vector. $\bar{n}$ is a $N \cdot N_r$ dimensional vector of additive white Gaussian noise. $\bar{I}$ is a $N \cdot N_r$ dimensional vector of interference and $\bar{H}$ is a $(N \cdot N_r) \times (N \cdot N_t)$ dimensional cyclic matrices. The GBSM channel proposed in Eq. 6 can be expressed as

$$\left[\bar{H}_{s,u}\right]_{CA} = \begin{bmatrix} H_{11} & H_{12} & \cdots & H_{1N_t} \\ H_{21} & H_{22} & \cdots & H_{2N_t} \\ \vdots & \vdots & \ddots & \vdots \\ H_{N_r1} & H_{N_r2} & \cdots & H_{N_rN_t} \end{bmatrix} \tag{10}$$

H_{ij} is a $N \times N$ dimensional discrete inverse Fourier Transform sub-matrix in Eq. 11. $H_{s,u}$ is diagonalized in other to obtain independence and maximum capacity for each channel. The diagonal sub-blocks are of $N \times N$ dimensional discrete Fourier Transform matrix in Eq. 12. The block diagonal matrices are shown as follows

$$F^{H(N_t)} = \begin{bmatrix} F_N^H & 0 & \cdots & 0 \\ 0 & F_N^H & \cdots & 0 \\ \vdots & \vdots & \ddots & \vdots \\ 0 & 0 & \cdots & F_N^H \end{bmatrix} \tag{11}$$

and

$$F^{(N_r)} = \begin{bmatrix} F_n & 0 & \cdots & 0 \\ 0 & F_n & \cdots & 0 \\ \vdots & \vdots & \ddots & \vdots \\ 0 & 0 & \cdots & F_n \end{bmatrix} \tag{12}$$

Equation 9 can then be re-written as

$$F^{(N_r)}\bar{y} = F^{(N_r)}\bar{H}x + F^{(N_r)}\bar{n} + F^{(N_r)}\bar{I} \tag{13}$$

and further simplified as

$$Y = F^{(N_r)}\bar{H}F^{H(N_r)}X + Z \tag{14}$$

$Y = \left[Y_1^T, Y_1^T, ..., Y_{N_r}^T\right]^T$ is a $N_r \cdot N$ dimensional demodulated signal column vector. $X = \left[X_1^T, X_2^T, ..., X_{N_t}^T\right]^T$ is a $N_t \cdot N$ dimensional original transmitted signal column vector. Z is a combination of the noise vector and the interference. The frequency response of the $k-th$ subcarrier channel between the transmitting antenna i and the receiving antenna j will be $H_{ji}(k)$. The summation of N_t flat fading signals will constitute the demodulation signal on the $k-th$ subcarrier of each receiving antenna j [19].

$$Y_j(k) = \sum_{i=1}^{N_t} H_{ji}(k) \cdot X_i(k) + Z_j(k) \tag{15}$$

2.5 Successive Interference Cancellation in UAV Communication Network

In this section, we discuss how the interference within the UAV communication system can be reduced using the concept of successive interference cancellation (SIC). In SIC, a single user, in this example the UAV, is decoded uniquely at the base station, with all other users, such as other UAVs, base stations, and user equipment, being treated as interference. This decision is done by the decision region ρ. Single user matching filters are used to make these decisions, which ignores the existence of interference [35]. At the receiver, the interfering signal can be replicated and removed from the received waveform. This process is continued until all of the information streams sent have been demodulated. If the decision made was accurate, this procedure cancels the interfering signal [35]. Figure 3 depicts a two-user SIC being employed by the base station in the downlink scenario.

In Fig. 3, supposing UAV 2 is demodulated by its matched filter:

$$y_2 = sgn(Y_2) \tag{16}$$

The signal of user 2 with y_2 is remodulated to obtain $A_2 y_2 s_2(t)$ and then subtracted from the received signal to yield

$$\hat{y}(t) = Y(t) - A_2 y_2 s_2(t) \tag{17}$$

$$= A_1 y_1 s_1(t) + A_2 (\hat{y}_2 - y_2) s_2(t) + n(t) \tag{18}$$

Using the matched filter for s_1 to process $\hat{y}$, we obtain

$$y_1 = sgn(\{\hat{y}, s_1\}) \tag{19}$$

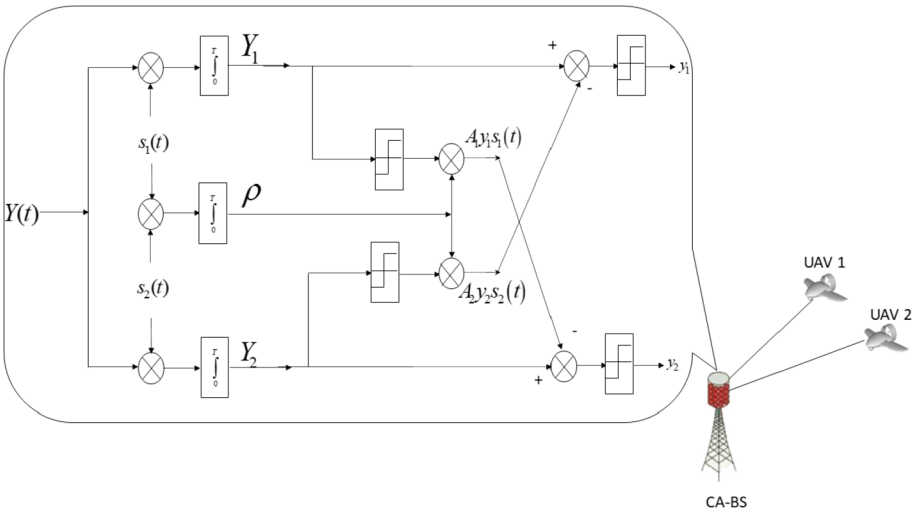

Fig. 3. CA-BS performing a two-user SIC

$$= sgn(y_1 - A_2 y_2 \rho) \tag{20}$$

$$= sgn\left(y_1 - A_2 \rho sgn\left(Y_2\right)\right) \tag{21}$$

$$= sgn\left(A_1 \hat{y}_1 + A_2\left(\hat{y}_2 - y_2\right)\rho + \sigma\left(n, s_1\right)\right) \tag{22}$$

3 Numerical Results

In this section, we provide the simulated results to evaluate our proposed system for the UAV communication network. The experimental environment of this paper is based on MATLAB 2018a. For this study, we demonstrate how the capacity and BER of a signal are affected in UAV communication networks when MIMO-OFDM together with SIC are employed. Also, SINR will be used to analyze the impact on the performance evaluation metrics. Table 1 shows the simulation parameters used for the experiment.

For the cylindrical array base stations, we considered three circular arrays each in the zenith domain. Where each circular array constitutes two antennas and also an instance where each circular array constitutes four antennas. For the 3-D channel modeling, we set $\theta_{tilt} = 95°$, $\theta = 15°$, and $\phi = 70°$ as described in [32]. The AoA and AoD are drawn from the Laplacian distribution. The results in Fig. 4 shows that an increase in the number of antennas increases the capacity with increasing SINR. With interference within the UAV communication network, the channel capacity reduces generally regardless of the number of antennas used in the UAV communication network. When SIC was used in the communication network, the channel capacity improved as it reduced the

Table 1. UAV simulation parameters

Description	Parameter	Value
UAV transmit power	P_s	5 W
Path loss exponent	v	3
Fixed distance between base stations	d_s	20 m
Interfering signal power	p_i	5 W
Modulation scheme		16QAM
Number of OFDM samples used	N_s	100000
Downward tilt of the antenna	θ_{tilt}	95°
Vertical beamwidth	θ	15°
Horizontal beamwidth	ϕ	70°

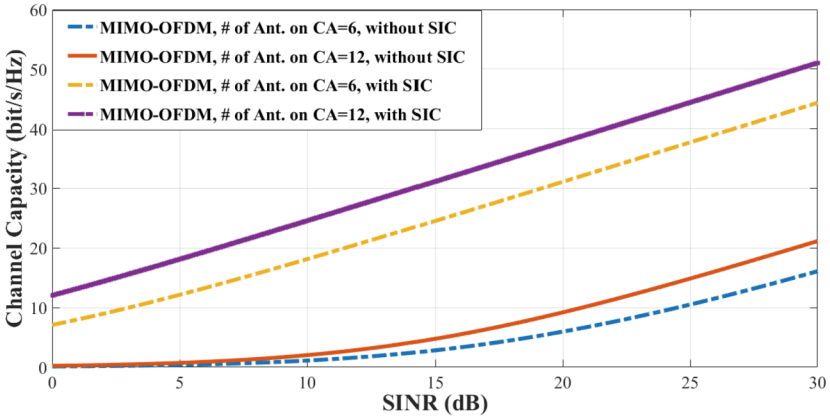

Fig. 4. Capacity vs SINR of CA MIMO-OFDM with and without SIC

interference with the network. For the BER analysis, BER in the UAV communication network was improving with a corresponding increase in the number of antennas used and increasing SINR. However, in Fig. 5 it was observed that beyond SINR of about 25 dB, it was observed that the BER no longer reduced with increasing SINR. This is a result of the irreducible error floor due to the interference. When SIC was employed in the experiment it could be observed from Fig. 5 that the irreducible error floor had been reduced and that an increase in SINR continued to give a better BER for our proposed system. Table 2 shows a comparison of existing literature and our proposed network.

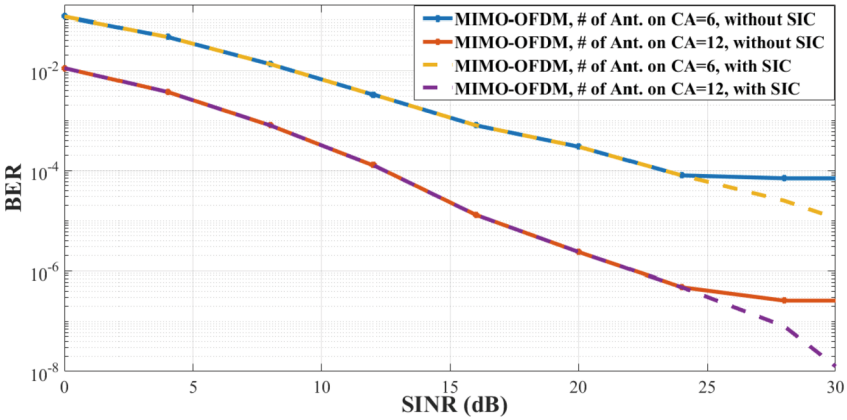

Fig. 5. BER vs SINR of CA MIMO-OFDM with and without SIC

Table 2. Comparison of prior work and proposed system

Reference	Channel	Interference	SIC	Capacity(bits/s/Hz)	BER
[19]	CBSM	No	No	20	10^{-2}
Proposed system	GBSM	Yes	Yes	30	10^{-4}

4 Conclusion

Improving transmission quality in UAV communication networks has been of major concern in UAV communication. In this research, we proposed the use of MIMO-OFDM in UAV communication networks. The antenna of the base stations was modelled as a cylindrical array with the channel GBSM. Also, we presented an interference model in the channel to the impact of interference on the communication system. Results indicated that as the number of antennas increases in the UAV communication network, so does the channel capacity and BER of the network increase with increasing SINR. This trend continues till the irreducible error floor point where an increase in SINR no longer improves the BER. Successive Interference Cancellation (SIC) is introduced such that the interference within the system will be mitigated and reduce the irreducible error floor.

References

1. Zeng, Y., Zhang, R., Lim, T.J.: Wireless communications with unmanned aerial vehicles: opportunities and challenges. IEEE Commun. Mag. **54**(5), 36–42 (2016). https://doi.org/10.1109/MCOM.2016.7470933
2. Al-Hourani, A., Kandeepan, S., Jamalipour, A.: Modeling air-to-ground path loss for low altitude platforms in urban environments. In: 2014 IEEE Global Communications Conference, pp. 2898–2904 (2014). https://doi.org/10.1109/GLOCOM.2014.7037248

3. Dan, G., Michel, A.H.: Drone Sightings and Close Encounters: An Analysis. Center for the Study of the Drone, Bard College, Annandale-on-Hudson, NY, USA (2015)
4. Mozaffari, M., Saad, W., Bennis, M., Nam, Y.-H., Debbah, M.: A tutorial on UAVs for wireless networks: applications, challenges, and open problems. IEEE Commun. Surv. Tutor. **21**(3), 2334–2360 (2019). https://doi.org/10.1109/COMST.2019.2902862
5. Valavanis, K.P., VachtsevanosValavanis, G.J. (eds.): Handbook of Unmanned Aerial Vehicles, vol. 2077. Springer, Dordrecht (2015). https://doi.org/10.1007/978-90-481-9707-1
6. Beard, R.W., McLain, T.W.: Small Unmanned Aircraft. Princeton University Press (2012). https://doi.org/10.1515/9781400840601
7. Puri, A.: A survey of unmanned aerial vehicles (UAV) for traffic surveillance. Department of Computer Science and Engineering, University of South Florida, pp. 1–29 (2005)
8. Mozaffari, M., Saad, W., Bennis, M., Debbah, M.: Mobile Unmanned Aerial Vehicles (UAVs) for energy-efficient internet of things communications. IEEE Trans. Wireless Commun. **16**(11), 7574–7589 (2017). https://doi.org/10.1109/TWC.2017.2751045
9. Atoev, S., Kwon, O.H., Lee, S.H., Kwon, K.R.: An efficient SC-FDM modulation technique for a UAV communication link. Electronics **7**(12), 352 (2018)
10. Ehichioya, D., Golriz, A.: Performance comparison of OFDM and DSSS on aeronautical channels. International Foundation for Telemetering (2009)
11. Geraci, G., Garcia-Rodriguez, A., Giordano, L.G., Lopez-Perez, D., Bjoernson, E.: Supporting UAV Cellular Communications through Massive MIMO. In: 2018 IEEE International Conference on Communications Workshops (ICC Workshops), pp. 1–6 (2018). https://doi.org/10.1109/ICCW.2018.8403630
12. Geraci, G., Garcia-Rodriguez, A., Hassan, M., Ding, M.: UAV Cellular Communications: Practical Insights and Future Vision (2018)
13. ENTT DOCOMO Inc., Ericsson. New SID on enhanced support for aerial vehicles. 3GPP RP-170779 RAN#75, Mar., 2017
14. LG Electronics. Interference mitigation for aerial vehicle. 3GPP R1–1718267, # 90bis, October 2017
15. Sony. Height parameter and CRS collision for aerial vehicle. 3GPP R1–1718267, #90bis, October 2017
16. Sequans Communications. Interference mitigation for aerial vehicle. 3GPP R1–1718267 #90bis, August 2017
17. Marzetta, T.L.: Noncooperative cellular wireless with unlimited numbers of base station antennas. IEEE Trans. Wireless Commun. **9**(11), 3590–3600 (2010). https://doi.org/10.1109/TWC.2010.092810.091092
18. Rusek, F., et al.: Scaling Up MIMO: opportunities and challenges with very large arrays. IEEE Signal Process. Mag. **30**(1), 40–60 (2013). https://doi.org/10.1109/MSP.2011.2178495
19. Tan, X., Su, S., Guo, X., Sun, X.: Application of MIMO-OFDM technology in UAV communication network. In: 2020 2nd World Symposium on Artificial Intelligence (WSAI), pp. 1–4 (2020). https://doi.org/10.1109/WSAI49636.2020.9143309
20. Gupta, A.K., Chockalingam, A.: Performance of MIMO modulation schemes with imaging receivers in visible light communication. J. Lightwave Technol. **36**(10), 1912–1927 (2018). https://doi.org/10.1109/JLT.2018.2795698

21. Al-Askery, A.J., Tsimenidis, C.C., Boussakta, S., Chambers, J.A.: Performance analysis of coded massive MIMO-OFDM systems using effective matrix inversion. IEEE Trans. Commun. **65**(12), 5244–5256 (2017). https://doi.org/10.1109/TCOMM.2017.2749370
22. Sun, X., Gao, X., Li, G.Y., Han, W.: Single-site localization based on a new type of fingerprint for massive MIMO-OFDM systems. IEEE Trans. Veh. Technol. **67**(7), 6134–6145 (2018). https://doi.org/10.1109/TVT.2018.2813058
23. Zhang, W., Li, H., Kong, W., Fan, Y., Cheng, W.: Structured compressive sensing based block-sparse channel estimation for MIMO-OFDM systems. Wireless Pers. Commun. **108**(4), 2279–2309 (2019). https://doi.org/10.1007/s11277-019-06522-8
24. Ampoma, A.E., Wen, G., Huang, Y., Gyasi, K.O., Tebe, P.I., Ntiamoah-Sarpong, K.: Spatial correlation models of large-scale antenna topologies using maximum power of offset distribution and its application. IEEE Access **6**, 36295–36304 (2018). https://doi.org/10.1109/ACCESS.2018.2846260
25. Document 3GPP TR 36.873 v12.0.0. Study on 3D channel model for LTE. September 2014
26. Zheng, K., Ou, S., Yin, X.: Massive MIMO channel models: a survey. Int. J. Antennas Propag. **2014** (2014). Article no. 848071
27. Liu, G., Hou, X., Wang, F., Jin, J., Tong, H., Huang, Y.: Achieving 3D-MIMO with massive antennas from theory to practice with evaluation and field trial results. IEEE Syst. J. **11**(1), 62–71 (2017)
28. Sipus, Z., Bosiljevac, M., Skokic, S.: Mutual coupling analysis of cylindrical waveguide arrays using hybrid SD-UTD method. In: Proceedings of the IEEE Antennas Propagation Society International Symposium, vol. 1A, pp. 155–158, July 2005
29. Pluzhnikov, A.D., Pribludova, E.N., Ryndyk, A.G.: Cylindrical array as a means of the clutter suppression via scanning acceleration and spacetime signal processing. In: Proceedings of the 44th European Microwave Conference, pp. 1864–1867, Rome, Italy (2014)
30. Kanatas, A.G., Nikita, K.S., Mathiopoulos, P.: New Direction in Wireless Communications Systems: from mobile to 5G. ISBN: 978-1-4987-8545-7
31. Study on 3D Channel Model for LTE, document 3GPP TR 36.873 V12.0.0, September 2014
32. Nadeem, Q.U.A., Kammoun, A., Debbah, M., Alouini, M.S.: Spatial correlation characterization of a uniform circular array in 3D MIMO systems. In: Proceedings of the 17th International Workshop Signal Process. Advanced Wireless Communication (SPAWC), pp. 1–6, Edinburgh, U.K. (2016)
33. Nadeem, Q.U.A., Kammoun, A., Debbah, M., Alouini, M.S.: 3D massive MIMO systems: modeling and performance analysis. IEEE Trans. Wireless Commun. **14**(12), 6926–6939 (2015)
34. Kammoun, A., Khanfir, H., Altman, Z., Debbah, M., Kamoun, M.: Preliminary results on 3D channel modeling: from theory to standardization. IEEE J. Sel. Areas Commun. **32**(6), 1219–1229 (2014)
35. Verdu, S.: Multiuser detection, pp. 344–368, ISBN:0-521-59373-5 (1998)